

# COMPUTER SIMULATION OF AIR INFILTRATION EFFECTS ON HEAT TRANSFER IN MULTILAYERED WALLS

Chebil S.<sup>1,2</sup> Galanis N.<sup>1</sup> Zmeureanu R.<sup>2</sup>

<sup>1</sup> Université de Sherbrooke, Sherbrooke, Québec [Schebil@cbs-engr.concordia.ca](mailto:Schebil@cbs-engr.concordia.ca) [Nicolas.galanis@gme.usherb.ca](mailto:Nicolas.galanis@gme.usherb.ca) <sup>2</sup> Concordia University, Montreal, Quebec [Zmeur@cbs-engr.concordia.ca](mailto:Zmeur@cbs-engr.concordia.ca)

## ABSTRACT

Significant thermal coupling can occur between the air infiltration and wall layers, thereby modifying the heat transmission in building envelopes. The purpose of this study is to obtain a better understanding of the air infiltration effects on the heat transfer in typical multilayered walls. This paper presents a numerical model of transient 3-D heat transfer phenomena in a wall system to evaluate the effect of outside air moving within cavities, for instance around the insulation layer. A finite difference method is used. Simulated temperature variations and heat flux responses at the inner and outer sides are presented for different wall configurations. The effect of the air leakage rate on the heat flux is discussed.

## INTRODUCTION

Infiltration is one of the major contributors to heating and cooling costs of buildings, especially in houses where infiltration typically constitutes about one-third of the total space-conditioning load [1]. Currently, the air in/exfiltration rate of a house can be predicted. However, the effect of these airflows on the thermal performance of building envelopes has not been thoroughly analysed.

A number of studies have treated the effects of air movement on the heat flow through insulator systems [2-4]. The air intrusion occurs either through insulation pores or through air cavities along insulation interfaces. Experimental and numerical studies have shown that convective airflow degrades the effective thermal resistance of air-permeable-insulations [5]. Powell et al. [6] reviewed the studies about the influence of the air movement on the effective thermal resistance of porous insulation under various conditions.

The effect of air intrusion on the thermal performance of a wall depends on many factors such as:

- Rate of air movement induced into the wall;
- Location and dimensions of cavities;
- Dominant heat transfer mechanism: natural or forced convection, radiation, and conduction;

- Material characteristics (e.g., porosity, thickness, thermal conductivity);
- Natures of the air flow, i.e., through the insulation layer, or through air cavities.

## MODEL DESCRIPTION

Figure 1 shows a horizontal section of a multilayered wall system, typical in North America. The brick layer ① is followed by an air gap ② and plywood sheathing ③. Then, generally comes the insulation layer ⑤ standing between the vertical and horizontal wood studs ⑥. The interior side of the wall is covered with a gypsum board layer ④. When the plywood and gypsum board are not well connected with the studs (due to deformation or installation defects), air cavities may exist around the different interfaces. Cavity positions on the wall are described on figure 1 (layer ④: Cav1 to Cav5; layer ⑦: Cav10 to Cav14). Cavities between the stud/insulation interfaces (Cav6 to Cav9) may also be present. All these cavities might be the possible leakage routes for the outside cold air when infiltration occurs.

The following coordinates system is selected: OX is normal to the wall, OY is vertical, and OZ is horizontal along the wall.

Due to temperature difference between inside ( $T_{int}$ ) and outside ( $T_{ext}$ ), the multilayered wall is subject to different heat transfer mechanisms:

1. Heat conduction in each material.
2. Convection on both exterior and interior sides.
3. Natural convection occurring inside the air gaps of layer ② and the cavities Cav1 to Cav14.
4. Radiation between the surfaces of different layers.
5. When air flows from outside into the conditioned space (infiltration), forced convection might occur inside the cavities.
6. The top, bottom, left and right sides of the wall are subjected to constant fluxes  $Q_{top}$ ,  $Q_{bottom}$ ,  $Q_{left}$  and  $Q_{right}$  ( $W/m^2$ ). In this paper, the adiabatic conditions are assumed on the perimeter of the considered wall ( $Q_{top}=Q_{bottom}=Q_{left}=Q_{right}=0 W/m^2$ ).



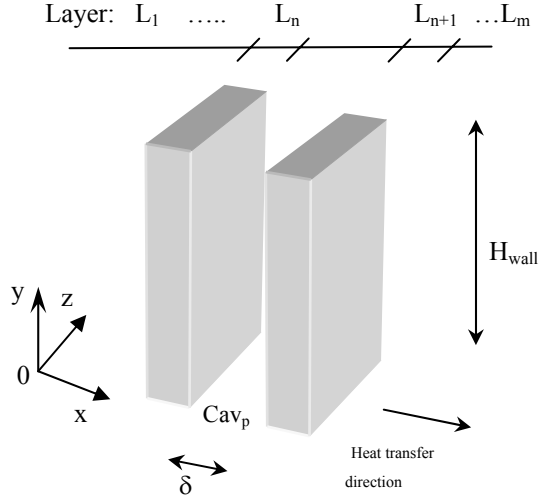


Figure 2: Air cavity between two layers

The correlation of Nusselt number developed by Jakob for vertical enclosed space was used [9]:

$$Nu_{\delta} = 0.18 * Gr^{0.25} * (H_{wall}/\delta)^{1/9} \quad (7)$$

When  $\delta$  and the thermal conductivity of the air ( $K_{air}$ ) at local mean temperature  $(T_{ln} + T_{ln+1})/2$  are known, the convective heat coefficient “ $h_{cavp\_conv}$ ” is defined:

$$h_{cavp\_conv} = Nu_{\delta} \cdot K_{air} / \delta \quad (8)$$

The boundary condition at surfaces of layer  $L_n$  and  $L_{n+1}$  is defined as follow:

at surface of layer  $L_n$ :

$$-K_{ln} \partial T / \partial x_{(x=X_{ln}, y, z, t)} = hcav_p (T_{ln} - T_{ln+1}) \quad (9)$$

at surface of layer  $L_{n+1}$ :

$$-K_{ln+1} \partial T / \partial x_{(x=X_{ln+1}, y, z, t)} = hcav_p (T_{ln+1} - T_{ln}) \quad (10)$$

$hcav_p$  is the total heat transfer coefficient within the cavity delimited by the layers  $L_n$  and  $L_{n+1}$ , taking into account both convection and radiation heat transfer:

$$hcav_p = h_{cavp\_rad} + h_{cavp\_conv} \quad (11)$$

For narrow air spaces, defined as those for which the product of the temperature difference (in Kelvin) and the cube of the space thickness (in millimeters) is less than 27000 (for heat flow horizontally or downward), or less than 9000 (for heat flow upward), convection is practically suppressed [10]. This case was not yet implemented in the numerical model.

### Heat flow through the wall with infiltration

In case when air infiltration occurs, the heat and mass transfer phenomena are coupled.

The different possible airflow routes through the wall system, which are considered in this paper, are showed with arrows in Figure 1.

#### Assumptions:

1. Every cavity has a fixed thickness along the entire wall height.
2. The airflow coming into the wall passes by the cavity Cav1.
3. At the entrance of Cav1, the air temperature is equal to the outdoor air temperature ( $T_{out}$ ).
4. No infiltration occurs in layer 2 and in cavities 5 (Cav5) and 14 (Cav14).
5. Although the airflow can occur either through the material pores or through air cavities along insulation interfaces, in this study, only infiltration along insulation interfaces is considered.
6. Mass flow rates for each cavity are fixed.

In this study, the airflow in each cavity is considered to be one-dimensional: in the direction of OZ for Cav1 to Cav5 and Cav10 to Cav14, and in the direction OX for Cav6 to Cav9.

The modeling of coupled heat and mass transfer phenomena is presented as an example for Cav2 (Figure 3). The energy conservation law applied to the dashed control volume  $\Delta z \cdot \delta_{cav2} \cdot \Delta y$  ( $\Delta y$  is set in a perpendicular plan), leads to:

$$\begin{aligned} M_{cav2} \cdot Cp_{air} \cdot (T_{cav2(k)} - T_{cav2(k-1)}) = \\ \Delta y \cdot \Delta z \cdot h_{cav2} \cdot [(T_{(i,j,k)} + T_{(i,j,k-1)})/2 - (T_{cav2(k)} + T_{cav2(k-1)})/2] + \\ \Delta y \cdot \Delta z \cdot h_{cav2} \cdot [(T_{(i+1,j,k)} + T_{(i+1,j,k-1)})/2 - \\ (T_{cav2(k)} + T_{cav2(k-1)})/2] \end{aligned} \quad (12)$$

$M_{cav2}$  is the air mass flow rate entered in the cavity Cav2.

When air flows in a cavity  $n$ , the convective heat transfer coefficient  $hcav_n$  can be determined from the Nusselt number correlation for crack flow [11]:

$$hcav_n = Nu_{f\_n} \cdot K_{air} / D_{h\_n} \quad (13)$$

$D_{h\_n}$  : Hydraulic diameter for cavity  $n$  (m).

$Nu_{f\_n}$ : Forced convection Nusselt number for cavity  $n$ .

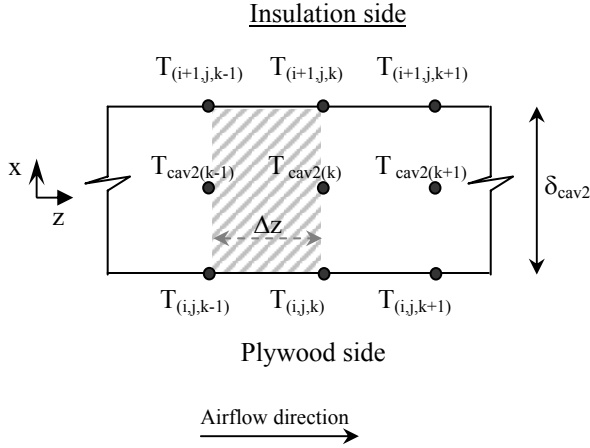


Figure 3: Coupling between heat transfer and air infiltration in cavity Cav2

In the case of laminar flow ( $Re < 2000$ ), the following Nusselt number correlations for forced convection ( $Nu_f$ ) is used [11]:

$$Nu_f = 1.85 (Re.Pr.D_h/H_{wall})^{1/3} \quad \text{if } Re.Pr.D_h/H_{wall} > 70$$

$$Nu_f = 7.54 \quad \text{if } Re.Pr.D_h/H_{wall} \leq 70 \quad (14)$$

### Solution Procedure

A numerical model of transient 3-D conduction heat transfer in a wall system was developed using the finite difference method. A fully implicit scheme was used for the discretization of Fourier's equation.

As an example, assuming a one material layer, one can obtain the following equations:

- On the exterior surface:

$$[(\Delta x \Delta y \Delta z / (2k \Delta t)) + (h_{ext} \Delta y \Delta z / K) + (\Delta y \Delta z / \Delta x) + (\Delta x \Delta z / \Delta y) + (\Delta x \Delta y / \Delta z)] T_{i,j,k}^{t+1} =$$

$$(h_{ext} \Delta y \Delta z / K) T_{ext}^{t+1} + (\Delta y \Delta z / \Delta x) T_{i+1,j,k}^{t+1} +$$

$$(\Delta x \Delta z / (2\Delta y)) T_{i,j-1,k}^{t+1} + (\Delta x \Delta z / (2\Delta y)) T_{i,j+1,k}^{t+1} +$$

$$(\Delta x \Delta y / (2\Delta z)) T_{i,j,k-1}^{t+1} + (\Delta x \Delta y / (2\Delta z)) T_{i,j,k+1}^{t+1} +$$

$$(\Delta x \Delta y \Delta z / (2k \Delta t)) T_{i,j,k}^t \quad (15)$$

- Within the wall

$$[(\Delta x \Delta y \Delta z / (k \Delta t)) + (2\Delta y \Delta z / \Delta x) + (2\Delta x \Delta z / \Delta y) + (2\Delta x \Delta y / \Delta z)] T_{i,j,k}^{t+1} =$$

$$(\Delta y \Delta z / \Delta x) T_{i-1,j,k}^{t+1} + (\Delta y \Delta z / \Delta x) T_{i+1,j,k}^{t+1} +$$

$$(\Delta x \Delta z / \Delta y) T_{i,j-1,k}^{t+1} + (\Delta x \Delta z / \Delta y) T_{i,j+1,k}^{t+1} +$$

$$(\Delta x \Delta y / \Delta z) T_{i,j,k-1}^{t+1} + (\Delta x \Delta y / \Delta z) T_{i,j,k+1}^{t+1} +$$

$$(\Delta x \Delta y \Delta z / (k \Delta t)) T_{i,j,k}^t \quad (16)$$

- On the interior surface

$$[(\Delta x \Delta y \Delta z / (2k \Delta t)) + (h_{int} \Delta y \Delta z / K) + (\Delta y \Delta z / \Delta x) + (\Delta x \Delta z / \Delta y) + (\Delta x \Delta y / \Delta z)] T_{i,j,k}^{t+1} =$$

$$(h_{int} \Delta y \Delta z / K) T_{int}^{t+1} + (\Delta y \Delta z / \Delta x) T_{i-1,j,k}^{t+1} +$$

$$(\Delta x \Delta z / (2\Delta y)) T_{i,j-1,k}^{t+1} + (\Delta x \Delta z / (2\Delta y)) T_{i,j+1,k}^{t+1} +$$

$$(\Delta x \Delta y / (2\Delta z)) T_{i,j,k-1}^{t+1} + (\Delta x \Delta y / (2\Delta z)) T_{i,j,k+1}^{t+1} +$$

$$(\Delta x \Delta y \Delta z / (2k \Delta t)) T_{i,j,k}^t \quad (17)$$

Where  $T^t$  is the present temperature at time  $t$ , and  $T^{t+1}$  denotes the future temperature at time  $t + \Delta t$ . A one-hour time step was chosen during the study presented in this paper.  $\Delta x$ ,  $\Delta y$  and  $\Delta z$  are the dimensions of the control volume in Cartesian coordinates.

The Tri-Diagonal-Matrix Algorithm (TDMA) method was used to solve the above linear discretized equations [12]. For faster convergence, OX was chosen as a line-by-line sweep direction [12].

## RESULTS AND ANALYSIS

### Preliminary validation: comparison with CTF method in the case of no air infiltration

For validation purposes, the numerical estimates of heat flow on the inside and outside surfaces were compared with results obtained with the conduction transfer function (CTF) method. Since this method does not consider air infiltration across the wall system and is restricted to one-dimensional heat transfer, the proposed model was applied to a wall without studs, composed only of parallel layers [7].

A typical wall (called **Wall A**) was selected from ASHRAE Handbook [7]. It is constructed of:

- 100 mm brick ( $K=0.72$  W/m.K;  $k=4.5E-7$  m<sup>2</sup>/s)
- 25 mm air gap
- 12 mm plywood ( $K=0.21$  W/m.K;  $k=1.1E-7$  m<sup>2</sup>/s)
- 140 mm fiberglass ( $K=0.046$  W/m.K;  $k=3.4E-6$  m<sup>2</sup>/s)
- 15 mm gypsum ( $K=0.727$  W/m.K;  $k=5.4E-4$  m<sup>2</sup>/s)
- The inside and outside surface resistances  $h_{int}$  and  $h_{ext}$  are assumed 8 and 34 W/m<sup>2</sup>.K respectively; with the CTF method,  $h_{gap}$  is considered constant (6 W/m<sup>2</sup>.K)
- For the numerical calculations, the wall was 2.5m high and 1.238m wide.

Heat flux on each node of the interior and exterior surfaces is calculated by the numerical method at every time step as follows:

$$Q_{\text{int}} = h_{\text{int}} \cdot (T_{\text{interior wall side}} - T_{\text{int}}) \quad (18)$$

$$Q_{\text{ext}} = h_{\text{ext}} \cdot (T_{\text{ext}} - T_{\text{exterior wall side}}) \quad (19)$$

$T_{\text{interior wall side}}$ : temperature on the interior wall surface.  
 $T_{\text{exterior wall side}}$ : temperature on the exterior wall surface.

For the time-varying outdoor temperature and solar radiation used for computation, the daily average heat flux at the wall surfaces is summarized in Table 1.

The numerical and CTF methods give similar results with errors of less than 3%. The estimated heat flux at the interior and exterior surfaces show a difference of less than 1%. This balance indicates that the energy conservation law is respected by the numerical model.

Table 1: Daily average heat flux through the wall.  
 Comparison of numerical and CTF methods

	CTF method	Numerical method
Heat flux at the interior ( $\text{W}/\text{m}^2$ )	-7.55	-7.36
Heat flux at the exterior ( $\text{W}/\text{m}^2$ )	NP*	-7.34

\* Not provided by CTF method

### Estimation of temperature profiles in the case of air infiltration

For analyzing the thermal effects of airflows in building structures, a wall system, called **Wall B** was considered. **Wall B** has the same configuration as **Wall A** with the addition of three vertical wood studs (140 mm thick and 38 mm large;  $K=0.21 \text{ W}/\text{m}\cdot\text{K}$ ;  $k=1.1\text{E}-7 \text{ m}^2/\text{s}$ ); two studs are installed on the perimeter of the wall, while the third stud is in the middle of the wall. The distance between the studs is 600 mm.

The calculations have been carried out for steady-state conditions, with a sol-air temperature of  $-20 \text{ }^\circ\text{C}$  and an interior air temperature of  $+20 \text{ }^\circ\text{C}$ . Figure 4(a) shows the isothermals across the wall section when there is no infiltration. Since the wood studs have higher thermal conductivity than the fiberglass, the effect of thermal bridges is obvious.

Figure 4(b) illustrates the temperature profiles on the same wall when air infiltration is taken into consideration ( $M_{\text{cavi}}=0.001 \text{ kg}/\text{s}$ ). The outside cold air enters the cavity Cav1, at a temperature equal to the outdoor temperature ( $T_{\text{out}}=-20 \text{ }^\circ\text{C}$ ) and then follows the leakage route through cavities Cav1, Cav2, Cav3,

Cav4, Cav9, Cav13, Cav12, Cav11 and Cav10. All these cavities have a thickness of 3 mm. Cavities Cav5, Cav6, Cav7, Cav8 and Cav14 are closed.

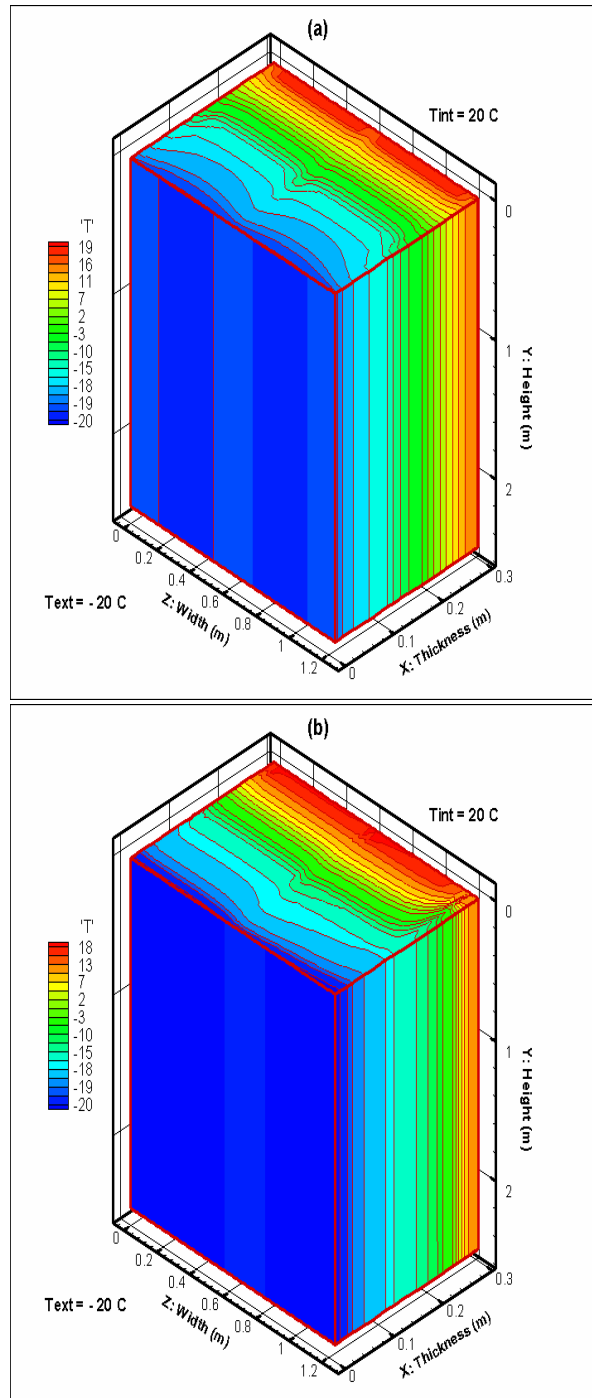


Figure 4: Wall temperature profiles without (a) and with infiltration (b)

The temperature profiles are clearly changed by the airflow. The cold air entering through the cavity Cav1 is warmed up as it flows through cavities Cav1, Cav2, Cav3 and Cav4. At the end of the first pass (as in a heat exchanger), the air is warmer, and the temperature of the neighboring nodes is also higher.

Table 2 shows the comparison between the average heat flux and temperature, respectively on both interior and exterior surfaces of the wall, without and with air infiltration ( $M_{cav1}=0.001$  kg/s). The intrusion of cold outside air has the result of lowering the temperature of the inside surface, and increasing the heat flux at the same surface (i.e., heat loss from interior air to wall). The balance between the heat loss at the inside surface ( $-22.50$  W/m<sup>2</sup>) and the heat loss at the outside surface ( $-10.55$  W/m<sup>2</sup>), equals (with an error less than 3.3%) the heat recovered by the cold infiltrated air ( $11.56$  W/m<sup>2</sup>). The air temperature leaving Cav10 is at  $15.79$  °C.

Table 2: Average heat flux and temperature at the inside and outside surfaces. Comparison between the cases without air infiltration and with air infiltration

	Without infiltration	With infiltration
Heat flux at the outside surface (W/m <sup>2</sup> )	-11.85	-10.55
Heat flux at the inside surface (W/m <sup>2</sup> )	-11.83	-22.50
Temperature of the outside surface (°C)	-19.65	-19.69
Temperature of the inside surface (°C)	18.52	17.19

### Estimation of the impact of air flow rates

**Wall B** was exposed to different infiltration airflow rates ( $M_{cav1} = 0.001, 0.005$  and  $0.009$  kg/s). The following path was considered: the outside air enters through the cavity Cav1 (at outdoor temperature) and then circulates through cavities Cav1, Cav2, Cav3, Cav4, Cav9, Cav13, Cav12, Cav11 and Cav10. Cavities Cav5, Cav6, Cav7, Cav8 and Cav14 are blocked. All cavities have the same thickness of 3 mm.

Table 3 illustrates the effect of the leakage rate on the heat loss through the inside and outside wall surfaces.

The wall behaves as a heat exchanger. The higher the air infiltration rate is, the higher is the heat recovery.

Hence, the heat flux at the inside surface is reduced when the air infiltration rate is increased.

Figures 5(a) and 5(b) present the variation of temperature of the outside surface ( $x=0$  m) and inside surface ( $x=0.292$  m), in the OZ direction.

Table 3: Effect of the airflow rate on the heat flux at the outside and inside surfaces

$M_{cav1}$ (kg/s)	Heat flux at the outside surface (W/m <sup>2</sup> )	Heat flux at the inside surface (W/m <sup>2</sup> )
0.001	-10.55	-22.50
0.005	-5.14	-64.36
0.009	-2.71	-98.54

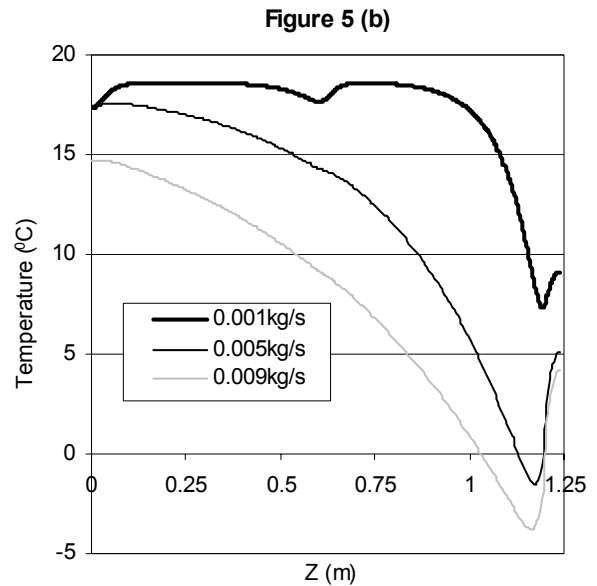
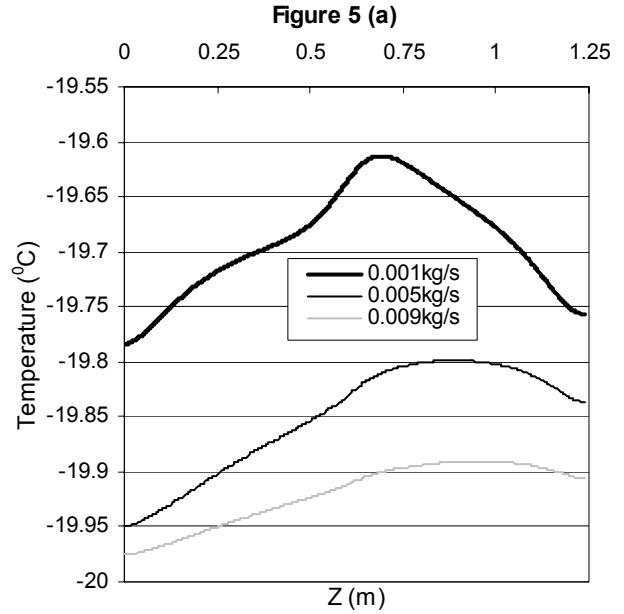


Figure 5: Temperature distribution at the outside (a) and inside surface (b) for different leakage rates (kg/s)

### Estimation of the impact of air leakage route

Several variables influence the heat exchange between the infiltrated airflow and the wall structure. The most significant parameters are flow rate and air leakage route [5]. To study the effect of the cavity opening positions through the Wall B, the following scenarios were proposed (see Figure 1):

- **S1:** Infiltration through cavities Cav1, Cav2, Cav3, Cav4, Cav9, Cav13, Cav12, Cav11 and Cav10.
- **S2:** Infiltration through cavities Cav1, Cav2, Cav3, Cav4 & Cav8, Cav9, Cav13, Cav12, Cav11 and Cav10.
- **S3:** Infiltration through cavities Cav1, Cav2 & Cav6, Cav7, Cav11 and Cav10.
- **S4:** Infiltration through cavities Cav1, Cav2, Cav3 & Cav7, Cav4, Cav9, Cav13, Cav12, Cav11 and Cav10.
- **S5:** Infiltration through all cavities except Cav5 and Cav14.

The leakage rate is assumed 0.005 kg/s and the cavities are 3 mm thick.

Figure 6 shows the temperature profile across the wall (in the OX direction), for the proposed routes. The profiles are taken in the wall centre (at  $y=1.25$  m;  $z=0.619$  m) passing through the middle stud.

With the first scenario **S1**, the airflow takes the longest route to reach the interior side of the wall. Cold air will recover heat all the way long reaching gradually the inner side temperature.

With the other scenarios, a short cut is created between the exterior and the interior of the wall. In that case, infiltration accelerates the “contact” between outdoor and indoor conditions, resulting in a less effective heat exchanger.

As illustrated in Figure 6, at the center of the wall, the inner side has the lowest wall temperature with scenario **S3**. Indeed, in that case the cold air reaches fast the inner layers, resulting in a considerable decrease of the interior surface temperature.

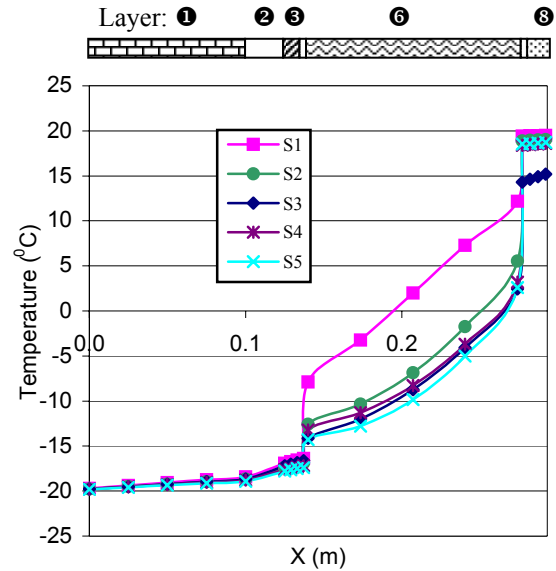


Figure 6: Temperature distribution across the wall under the proposed routes

### CONCLUSION AND FUTURE WORK

A numerical model was developed to evaluate the thermal coupling effect of heat transfer and air flow through a typical wall system. The results indicate that the air infiltration has a significant impact on both the temperature and the heat flux across the wall.

In future work, calculation of air mass flow rate in terms of a given pressure difference (between outside and inside) and physical characteristics of air cavities (thickness, length, etc.), will be implemented in the code. The case of exfiltration will be also examined. The air intrusion through the insulation pores will be added to the model. In addition, a window will be integrated to this wall structure. The three-dimensional simulation results will provide an accurate and more realistic picture of the entire wall/window thermal performances.

### ACKNOWLEDGEMENTS

The authors acknowledge the support received from Natural Sciences and Engineering Research Council of Canada.

## LIST OF SYMBOLS

$C_p$	Specific heat (J/kg.K)
$D_h$	Hydraulic diameter (m)
$g$	Acceleration due to gravity ( $m^2/s$ )
$Gr$	Grashof number
$h$	Convection coefficient ( $W/m^2.K$ )
$H$	Height (m)
$i,j,k$	i-th, j-th, k-th node on OX, OY and OZ directions, respectively
$I$	Solar radiation ( $W/m^2$ )
$I_{max}$	Maximum nodes on OX direction
$k$	Thermal diffusivity ( $m^2/s$ )
$K$	Thermal conductivity ( $W/m.K$ )
$M$	Mass flow of infiltrated air ( $kg/s$ )
$n, p$	n-th, p-th element
$Pr$	Prandtl number
$Q$	Heat flux ( $W/m^2$ )
$Ra$	Rayleigh number
$Re$	Reynolds number
$T$	Temperature ( $^{\circ}C$ )
$t$	Time (s)
$T_{ext}$	Sol-air temperature at the outside surface ( $^{\circ}C$ )
$T_{int}$	Interior air temperature ( $^{\circ}C$ )
$T_m$	Mean temperature of the two boundary facing surfaces ( $^{\circ}C$ )
$T_{out}$	Exterior temperature ( $^{\circ}C$ )
$T^t$	Temperature at time t ( $^{\circ}C$ )
$x,y,z$	Cartesian coordinates
$\Delta$	Time or distance increment
$\delta$	Gap/cavity thickness (m)
$\nabla$	Laplacien operator
$\alpha$	Absorptivity coefficient
$\beta$	Temperature coefficient of volume expansion (1/K)
$\nu$	Kinematic viscosity ( $m^2/s$ )
$\epsilon_{eff}$	Effective emissivity

## REFERENCES

- [1] Persily A., (1982), 'Understanding Air Infiltration in Homes', Report PU/CEES#129, Princeton University Centre for Energy and Environmental Studies, Princeton, NJ.
- [2] Wolf S., (1966), 'A theory for the Effects of Convective Air Flow Through Fibrous Thermal Insulation', *ASHRAE Transactions*, 72 Part 1, III 2.1-III 2.9.
- [3] Berlad A. L., Tutu N., Yeh Y., Jaung R., Krajewski R., Hope R. and Salzano F., (1978), 'Air Intrusion Effects on the Performance of Permeable Insulation Systems', *Thermal Insulation Performance*, 1988, D. McElroy and R. Tye, eds, ASTM STP 718, Oct., 181-194.
- [4] Lecompte J. G. N., (1987), 'The Influence of Natural Convection in Insulated Cavity on Thermal Performance of a Wall', *Insulation Materials Testing and Applications*, ASTM, FL.
- [5] Krarti M., (1994), 'Effect of Air Flow on Heat Transfer in Walls', *Journal of Solar Energy*, 116 35-42.
- [6] Powell F., Krarti M. and Tuluca A., (1989), 'Air Movement Influence on the Effective Thermal Resistance of Porous Insulation: A Literature Survey', *Journal of Thermal Insulation*, 12 239-251.
- [7] ASHRAE Fundamentals (1993).
- [8] Hollands K.G.T. and Konicek L., (1973), 'Experimental Study of the Stability of Differentially Heated Inclined Air Layers', *Int. J. Heat Mass Transfer*, 16 1467-1476.
- [9] Jakob M., (1949), *Heat Transfer Vol.1*, Wiley NY.
- [10] ASHRAE Fundamentals (2001).
- [11] Kohonen R., and M. Virtanen., (1987), 'Thermal coupling leakage flow and heating load of buildings'. *ASHRAE Transactions*, 93 2303-2318.
- [12] Patankar S. V., (1980), 'Numerical Heat Transfer and Fluid Flow', Hemisphere Publishing Corporation.